Environmental Engineering and Management Journal

May 2020, Vol.19, No. 5, 733-746
http://www.eemj.icpm.tuiasi.ro/; http://www.eemj.eu

"Gheorghe Asachi" Technical University of Iasi, Romania

CHARACTERIZATION AND PERFORMANCE OF POLYMER COMPOSITE MEMBRANES FOR THE REMOVAL OF HUMIC SUBSTANCES FROM WATER

Naziha Sid-Sahtout[1], Dalila Hank[1,2*], Amina Hellal[1]

[1]Laboratoire des Sciences et Techniques de l'Environnement, Ecole Nationale Polytechnique, Alger, Algérie
[2]Département Génie Rural, Ecole Nationale Supérieure Agronomique, Alger, Algérie

Abstract

This present study, investigates the performance of activated sardine scale powder (ASSP)/ Cellulose acetate (CA)/Polyvinylpyrrolidone (PVP) and powdered activated carbon (PAC)/ Cellulose acetate (CA) / Polyvinylpyrrolidone (PVP) composites membranes prepared by phase inversion for the elimination of humic substances (HS) from aqueous solutions. The materials and composites membranes were characterized by FTIR, XRD, SEM analyses. Overall, the results exhibit the higher performance of ASSP /CA/ PVP composite membrane than PAC /CA/ PVP composite membrane for the elimination of humic substances from water. Adsorption isotherm non-linear studies indicated that the two composites membranes can be successfully modeled by the Langmuir, Freundlich, and Temkin. The maximum monolayer adsorption capacity was found to be 31.00 mg/g and 23.32 mg/g for ASSP /CA/ PVP and PAC /CA/ PVP composites membranes, respectively. ASSP /CA/ PVP composite membrane seems to be a promising material for HS removal from aqueous solutions.

Keywords: activated carbon, adsorption, composite membrane, humic substance, phase inversion

Received: July, 2019; Revised final: October, 2019; Accepted: November, 2019; Published in final edited form: May 2020

1. Introduction

In water supply industry the natural organic matter (NOM) is a challenging problem, regardless to the taste and odours that are generated by its components; the human health is the real risk (Harfouchi et al., 2016; Williams et al., 2012; Zhao et al., 2015) . The NOM in surface and ground waters is present commonly as humic substances (Zhao et al., 2015) that are formed through the decomposition process of plants and animals, these substances constitute an active element of NOM which is constituted by two major components (Ulu et al., 2014), namely, fulvic acids and humic acids (Doulia et al., 2009). Consequently several water treatments to remove NOM have been adopted including the most common process which is coagulation and flocculation followed by sedimentation/flotation and filtration, adsorption, activated carbon filtration, ion exchange, and membrane filtration techniques (Hamdaoui and Naffrechoux, 2007; Williams et al., 2012).

Adsorption is a well-known method for separation equilibrium and is an efficient method for the removal of low concentrations of organic pollutants from large volumes of potable water, wastewater, and aqueous solutions (He et al., 2015; Mota et al., 2012). It has proved better than other techniques its flexibility, simplicity of design and easy implementation (Wei et al., 2015). Adsorption process has become quite attractive in the depollution of effluents loaded with inorganic or organic pollutants, due to the valorisation of natural materials, which are quite abundant and practically costless. Activated

*Author to whom all correspondence should be addressed: e-mail: dalila.hank@g.enp.edu.dz; Phone: +213 2152 53 01 / 03; Fax: +213 21 52 29 73

carbon is the most used adsorbent (Wei et al., 2015) because it has micro-pores, large surface area, and high adsorption capacity (Mota et al., 2012), but it is relatively expensive, and this limits applications to a large scale (Doulia et al., 2009; Wei et al., 2015).

Fish scale is an optional substitute adsorbent, due to the presence of numerous organic and inorganic components, mostly collagen and hydroxyapatite (Corami et al., 2007; Huang et al., 2011), such as hydroxyl, phosphate, carbonate, and amide (He et al., 2015). The formation of calcium sulphate was discussed in several works by reacting sulfuric acid with a natural calcium phosphate mineral such as apatite (Beddow et al., 2006; Koopman and Witkamp, 2000). This formation of calcium sulphate in aqueous solutions has three forms: gypsum ($CaSO_4$. $2H_2O$) hemihydrate ($CaSO_4.12H_2O$) and anhydride ($CaSO_4$) (Koopman and Witkamp, 2000).

Compared with the other separation processes, membrane processes have increased its importance by the low energy consumption, easy scale-up, less or no use of chemicals and non-harmful derivate formation (Arthanareeswaran et al., 2008; Rajeswari et al., 2015). Membranes can eliminate different pollutants using various processes such the separation mechanisms of impaction, diffusion, electrostatic interaction, hydrophobic property, and adsorption (Hwang et al., 2014). The composite membranes are frequently, in recent years, made by merging organic polymers with different organic or inorganic materials as a probable next generation membrane material (Celik et al., 2011).

The integration of organic/inorganic materials in organic polymers is well-known to increase polymer membranes capacity in permeability, porosity, and hydrophobicity and removal efficiency than those made of individual polymers (Arthanareeswaran et al., 2008; Hwang et al., 2013) Previous studies have reported that the preparation of composite membranes by phase inversion method can considerably improve the polymer membranes surfaces morphology and structures (Rahimpour and Madaeni, 2007; Saljoughi et al., 2009).

Phase inversion via immersion precipitation is the most largely applied to prepare asymmetric polymeric membrane (Mohammadi and Saljoughi, 2009). The substrate immersing in a coagulation bath, the solvent in the casting solution film is exchanged with a non-solvent in a precipitation medium and phase separation (Rahimpour and Madaeni, 2007; Saljoughi and Mohammadi, 2009). Several studies have examined the combination of organic polymer with inorganic materials like activated carbon (AC), alumina, silica, zirconia, Titania, etc. (Rajeswari et al., 2015). Hwang et al. (Hwang et al., 2013), work revealed that more the activated carbon (AC) is concentrated, results in bigger pores size, higher porosity of the AC/PPSU/PEI/PEG composite membrane an higher humic acids (HAs) removal efficiency. Similar results were reported for the CA/SiO_2 via phase inversion process by Arthanareeswaran et al. (2008). Mohamad Said et al. (2017) prepared new organic–inorganic membranes made by uniform polysufone-polyethyleneimine-silver-activated carbon (Psf-PEI-Ag-AC) and observed that AC content reaching 0.9 wt % showed a clear development of sponge structure and has the highest efficiency in elimination of heavy metals.

The objective of the present study is to explore the potential composites membranes structures and the performance of ASSP /CA/ PVP compared with the PAC /CA/ PVP composites membranes in removing humic substances from aqueous solution. The adsorbents will be characterized by FTIR, XRD and SEM. Batch experiments will be achieved for adsorption kinetics and isotherms. Langmuir, Freundlich end Temkin isotherms models will be used to analyse the adsorption data.

2. Material and methods

Humic Substances (HS) were purchased from HumatStar80-Almedsa Agrochimic-Algeria and used for all the adsorption studies. Chemical and physical properties of HS are reported in Table 1 (Harfouchi et al., 2016). The polymer used for forming membrane is Cellulose acetate (CA) (Sigma-Aldrich, USA), Average Mn ca. 50.000). Polyvinylpyrrolidone (PVP) with an average molecular weight of 10.000 g/mol (Sigma-Aldrich, China) was used as an additive. The 1-Methyl-2-pyrrolidone (NMP) with analytical purity of≥99.0% was purchased from Sigma-Aldrich (USA) and used as solvent. Distilled water was used as non-solvent agent.

2.1. Adsorbents

Sardine fish was bought at the market of El Harrach, Algeria. The scales were recovered and washed thoroughly in distilled water to remove salts and other substances and then dried at 105°C, for 24 h, ground and sieved to obtain a particle size≤320 μm.

Table 1. Chemical and physical properties of humic substances

Species	***Contents (%)***	***Species***	***Contents (%)***
Total organic matter	85%	Fulvic acid	15%
Total humic extract	80%	Magnesium	0.29%
Humic acid	65%	Calcium	1.3%
Solubility in water	100%	K_2O	8%
H_2O	15% max	Iron	0.3%

Table 2 shows the characteristics of powdered activated carbon F400 used in this study sieved to obtain a particle size≤320 µm.

Table 2. Powdered activated carbon characteristics (Hank et al., 2014)

Characteristic	***Value***
Origin	Bituminous oil
Iodine number (mg/g)	1050
Specific surface area (m^2/g)	1050-1200
Function of acid surface (mEq/g)	0.23

2.2. Activation of sorbent sardine scales powder (ASSP)

The activation of the sardine scales was carried out according to the method described by Müşerref et al. (Önal and Sarikaya, 2007).

In order to increase its adsorbent capacity, raw sardine scales powder (RSSP) was treated with sulfuric acid (40%) in the ratio 1/20 (m/v), in a water bath at 100°C under stirring for 6 hours. After that, the mixture was centrifuged and washed several times with hot distilled water to increase the pH to. Finally, it was dried for 24 hours in an oven at 105°C.

2.3. Membranes preparation

The membrane was prepared by phase inversion methods proposed by Cheng et al. (Saljoughi and Mohammadi, 2009). Pure membrane cellulose acetate (5.17wt %), polyvinylpyrrolidone (PVP, 1wt %) were dissolved into 1-Methyl-2-pyrrolidone (NMP). The solution was stirred continuously to obtain a uniform and homogeneous casting, then degassed about 24 hours to remove all air bubbles and kept away from direct light of the sun in order to slow down its aging process. The obtained solution was cast with 300 µm casting knife onto a glass plate, and then immediately immersed in a coagulation bath of distilled water at 25°C to complete the phase separation, where the solvent (NMP) and the non-solvent (distilled water) were exchanged. The membranes formed were then transferred to another container containing fresh distilled water to remove excess NMP and PVP. After 24 h, the membranes were ready to be tested.

For the other ASSP/CA/PVP and PAC/CA/PVP composite membranes, as shown in Fig. 1 and Fig. 2, respectively; the same steps were followed, until spreading with casting knife onto a glass plate then sprinkling 0.1g of activated sardine scales powder ASSP or PAC, waiting for a few seconds until the adsorbents is well fixed on the casting solution, and then immediately immersed in the coagulation bath.

2.4. Characterization

The elemental compositions of adsorbents were determined by FTIR and XRD analysis. The scanning electron microscopic (SEM) analysis was carried out for structural and morphological characteristics of native and composite membranes.

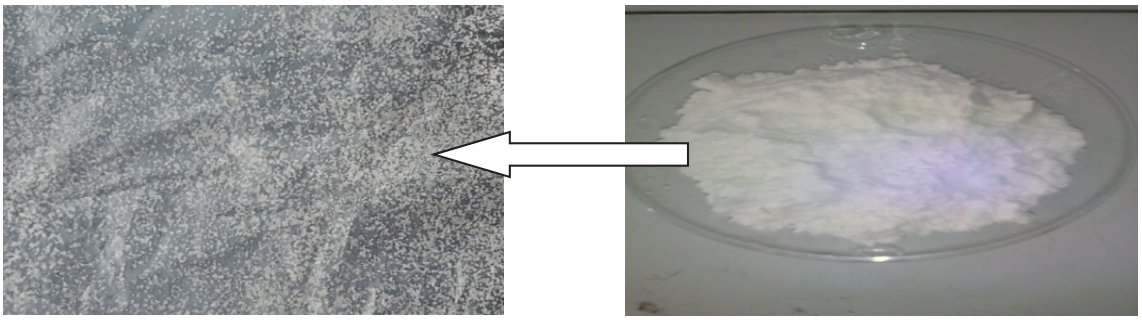

(a) (b)

Fig. 1. The morphology of: (a) the final activated sardine scale powder (ASSP) (≤ 320 µm) and (b) Membrane composite ASSP/CA/PVP

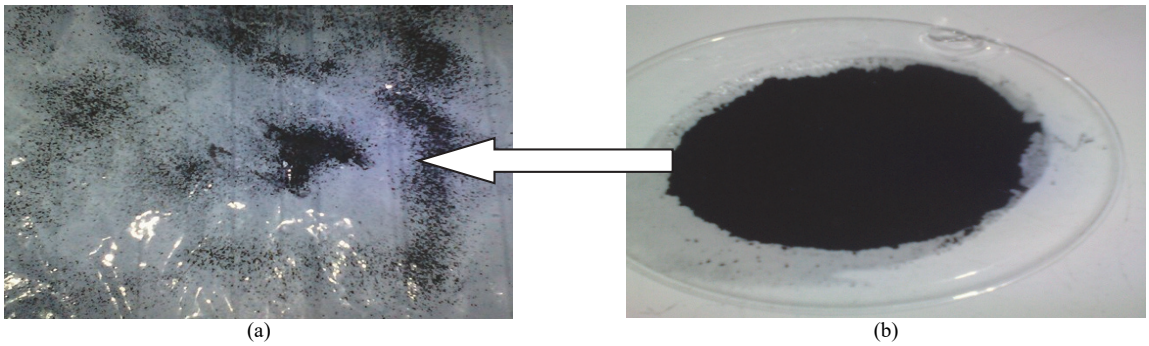

(a) (b)

Fig. 2. The morphology of: (a) the powdered activated carbon (PAC) (≤ 320 µm) and (b) Membrane composite PAC/CA/PVP

2.4.1. Fourier transforms infrared spectroscopy (FTIR)

The Fourier transform infrared spectroscopy was used to quantify the abundance of chemical functional groups (Corami et al., 2007) by a Perkin-Elmer spectrum using KBr pellets, in the range (400-4000 cm^{-1}).

2.4.2. X-ray diffraction (XRD)

The XRD analysis of the samples was carried out on a PANalyticalX'Pert pro diffractometer with a copper anode operating at 45kV and 40 Ma. The program scanned angles (2θ) from 4° to 70° with a step time of 10 s. The system of the XRD uses the principle of reflection of X-rays by crystalline materials.

2.4.3. Scanning electron microscopy (SEM)

The morphologies of the various adsorbents were characterized by a JEOL JSM -6360LV scanning electron microscope. The electron beams were sputtered on sample and images of adsorbents on varying resolutions were observed.

2.5. Adsorption study

Kinetic adsorption is required to understand mechanism of adsorption and define equilibrium time (Ghaedi et al., 2016). Adsorption experiments were carried out in batch system, by stirring at 180 rpm, 0.1 g of adsorbents (natural or activated ASSP, PAC, ASSP/CA/PVP and PAC/CA/PVP) at ambient temperature into 500 mL of a HS solution with initial concentration of 10 mg/L and pH 5.5 during 1440 min of contact time. The supernatant samples were taken at predetermined time intervals, prefiltered in a 0.45µm fibre to determine the HS concentration, by using an UVvis spectrophotometer (Shimadzu mini 1240) set at a wavelength of 254 nm. The HS uptake q_t (mg/g), was determined as follows (Eq. 1):

$$q_t = (C_0 - C_t) * V / m \quad (1)$$

where: C_0 is the initial concentration of HS solutions (mg/L), C_t is the HS solution concentration at any time t (mg/L), V is the solution volume (mL), and m is the adsorbent weight (g).

Adsorption isotherms were applied to describe the equilibrium performances of adsorbate uptake. The adsorption isotherms of HS on membranes were examined in a series of various concentrations (5, 6, 7 and 10 mg/L), adding a fixed mass of adsorbents (0.1 g) to 500 mL of HS solutions at ambient temperature and pH 5.5. The medium was stirring at 180 rpm for 240 min for ASSP/CA/PVP and 180 min for PAC/CA/PVP, to ensure the equilibrium.

The amount of HS adsorbed, q_e (mg/g), was obtained by Eq. (2):

$$q_e = (C_0 - C_e) * V / m \quad (2)$$

where: C_0 and C_e are the initial and equilibrium concentrations of HS (mg/L), respectively, V is the volume of solution (mL) and m is the amount of adsorbent used (g).

The supernatant samples were taken at predetermined time intervals, prefiltered in a 0.45 µm fiber to determine the HS concentration, by using a UV vis spectrophotometer (Shimadzu mini 1240) set at a wavelength of 254 nm (Harfouchi et al., 2016).

3. Results and discussion

3.1. FTIR Characterization

The FTIR has been applied to obtain information about structural and/or physic-chemical properties of the absorbents (RSSP, ASSP) and PAC, as shown in Fig. 3 (A and B) respectively.

It is clear from RSSP spectrum Fig. 3 (a) that the principal absorption band which occurs at 1164, 866 and 620 cm^{-1} is related to the triply degenerated asymmetric stretching mode (ν3), symmetric stretching mode(ν4) and asymmetric bending vibrations stretching respectively, that represent the vibration mode of the tetrahedral PO_4^{3-}(Harfouchi et al., 2016; Corami et al., 2007). Carbonate group (CO_3^{-2}) was identified by intense bands at 866 and 1557 cm^{-1} associated with out-of-plane bending mode and asymmetric stretching, respectively, which corresponds to carbonate anions substituted to phosphate ions in the hydroxyapatite lattice (Huang et al., 2011). The main absorption band at 3537cm^{-1}, corresponds to stretching vibrations of the bulk OH^- ions (Ghaedi et al., 2016; He et al., 2015; Mohamad Said et al., 2017). The results indicate that the RSSP is hydroxyapatite (Harfouchi et al., 2016; Huang et al., 2011).

In the ASSP spectra Fig. 3 (a), the strongest band that occurs near 1147 cm^{-1}, corresponds to symmetric stretching vibration mode ν1 of the tetrahedral SO_4^-.The spectrum contains a strong triple bands near 503, 608 and 679 cm^{-1}, which are related to the SO_4^- bending or lattice mode in the sulfate group (Pantos et al., 2009). The sharp band at 3455 cm-1 indicates hydroxyl (OH) stretching bands from water associated with the compound and a small peak at 2330 cm^{-1} is attributed to potassium bromide (KBr) (Harfouchi et al., 2016).

The PAC by FTIR spectrum illustrated in Fig. 3(b) shows H_2O bending vibration at 1384 cm^{-1} with integrated regions of oxygenated and aromatic carbon groups at 1638 cm^{-1}. The absorption bands at 2851 and 2917cm^{-1} indicates a symmetric and asymmetric stretching vibration of the CH_2 and CH_3 of the aliphatic chain (Hank et al., 2014).

3.2. XRD analysis

In the RSSP XRD patterns, Fig. 4(a) reveals fairly sharp and broad peaks indicating that the

material is poorly crystalline, identified as hydroxyapatite $Ca_{10}(PO_4)_6(OH)_2$ by the JCPDS74-0566 pattern (Abd El-aziz et al., 2017; Ramakrishnan et al., 2016) at diffraction angles (2θ) 25.91°, 31.81°, 32.21°, 32.91°, 39.81°, and 49.5°(Abd El-aziz et al., 2017).

The ASSP XRD patterns Fig. 4(b) show structural change in RSSP (hydroxyapatite) to calcium sulphate (anhydrite $CaSO_4$) after chemical activation by sulfuric acid (30% of H_2SO_4 at 100 °C) and identified as well crystalline in 2θ at angles 25.1°, 31.59°, 34.53°, 38.87°, 41.05°, and 43.59° (Kontrec et al., 2003). The XRD of PAC in Fig. 4(c) indicates clearly that the surface is principally amorphous in structure (Fernando et al., 2015; Maldhure and Ekhe, 2011; Mohamad Said et al., 2017). The three membranes XRD patterns in Fig. 4(d) show mainly amorphous structures. Despite the crystalline structure of the ASSP, the ASSP/CA/PVP composite membrane is amorphous due to poor quantity of ASSP.

3.3. Morphology analysis

The microstructure morphology of all the materials used in this study where examined using SEM. Figs. 5-8 and Fig. 5 (a, b and c) shows significant difference between RSSP, ASSP and PAC microstructure morphologies. The ASSP surface that seems agglomerated with irregular boundaries plates is more porous than RSSP surface which appears rough, the higher porosity of ASSP is due to the chemical activation with sulfuric acid (Doulia et al., 2009). The PAC surface reveals less pores comparing with ASSP (Fig.5 (c)).

The surface morphology and cross section in Figs. 6-8 present a typical asymmetric form with fingers like pores linked by sponge wall. In Fig. 6 the pure membrane appears smooth with small size pores (Arthanareeswaran et al., 2008). The SEM image in Fig. 7 represents ASSP membranes structures with particles uniformLy dispersed on surface with increased size pores and enhanced membrane porosity (Hwang et al., 2014) than the pure membrane.

In Fig. 8 The PAC particles appear agglomerated and irregularly dispersed, on the membrane surface and cross section, that caused a numerous of broken and collapsed pores formed mostly near the PAC particles which is created from the interfacial stresses between polymer and PAC (Wu et al., 2008).

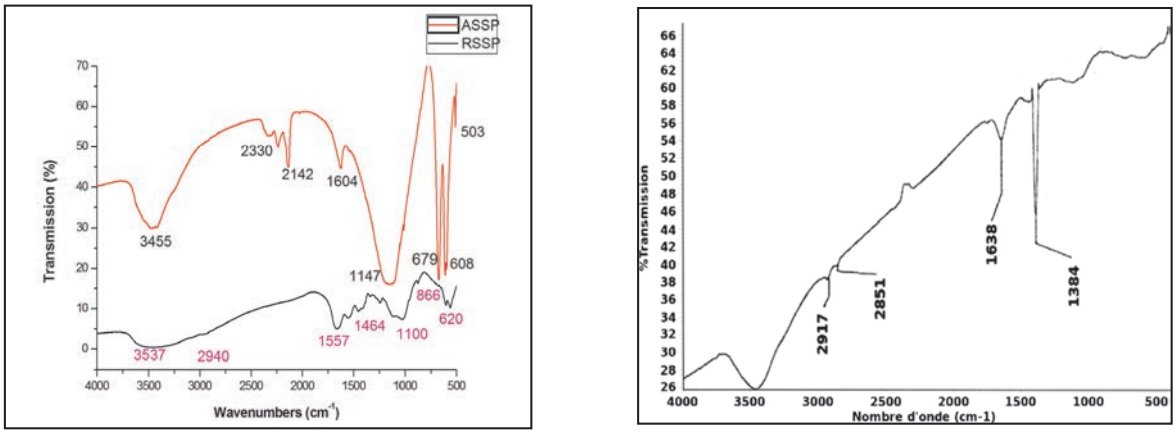

(a) (b)

Fig. 3. FTIR spectra of (a) ASSP and RSSP, (b) PAC (Hank et al., 2014)

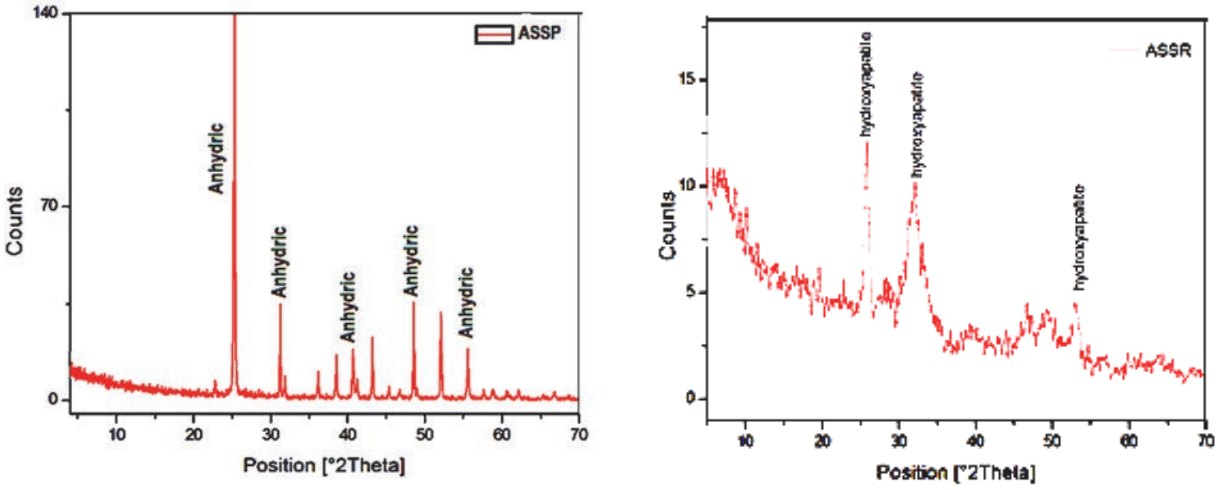

(a) (b)

3.4. Adsorption kinetics

The results of humic substances removal by RSSP, ASSP, ASSP/CA/PVP and PAC/CA/PVP are presented in Fig. 9 (A, B, C, D, E and F). Fig. 9(A), shows that the adsorption of the (SH) on ASSP is better than RSSP, the rates of HS elimination is important during the first fifteen minutes for brute and activated sardine scales. This can be explained by the fact that initially the adsorption sites are vacant (Basri et al., 2014) and easily accessible to the HS (Doulia et al., 2009). In Fig. 9 (B), the removal of HS on ASSP is higher than that obtained on ASSP/CA/PVP composite membrane. This is due to the larger ASSP surface area than composite membrane area.

The influence of the variation of the ASSP quantities in the composite membrane on the adsorption of HS (Fig. 9 (C)) indicates that the adsorption capacity increases with the increase of the ASSP mass from 0.05 g to 0.1 g, which increases the porosity (Hwang et al., 2013; Mohamad Said et al., 2017). According to Fig. 9(D), the results obtained show that the adsorption of the (SH) on ASSP is better than (PAC). This may be due to the porosity surface of the ASSP compared to the PAC.

The adsorption of HS on PAC in Fig. 9(E) is equal to the adsorption on PAC/CA/PVP composite membrane. It means that PAC retains its porosity or affinity with the humic substance in the membrane. Fig. 9(F), shows that the removal of HS on both composite membranes is better than that obtained on pure AC without any material. This is due to the incorporation of ASSP and PAC into pure CA that promoted large pores and increased porosity of the membrane.

3.5. Isotherms modeling

In general, adsorption isotherms provide information on the adsorption capacity, a description of the affinity and the adsorption energy between the adsorbate and the adsorbent (Hank et al., 2014; Rajeswari et al., 2015). Several adsorption equilibrium models have been broadly adopted to describe the liquid/solid phase adsorption comportment, such as the Langmuir, Freundlich and Temkin (Langmuir, 1918; Freundlich, 1906, 2018; Hank et al., 2014).

The Langmuir adsorption model (Langmuir., 1918; El Haouti et al., 2019; Techawongstien et al., 2012), assumes that the maximum sorption corresponds to a saturated monolayer of solute molecules on the adsorbent surface, without lateral interaction between the sorbet molecules. The Freundlich isotherms suppose that adsorption take place on a heterogeneous surface (Freundlich, 1906; El Haouti et al., 2019).

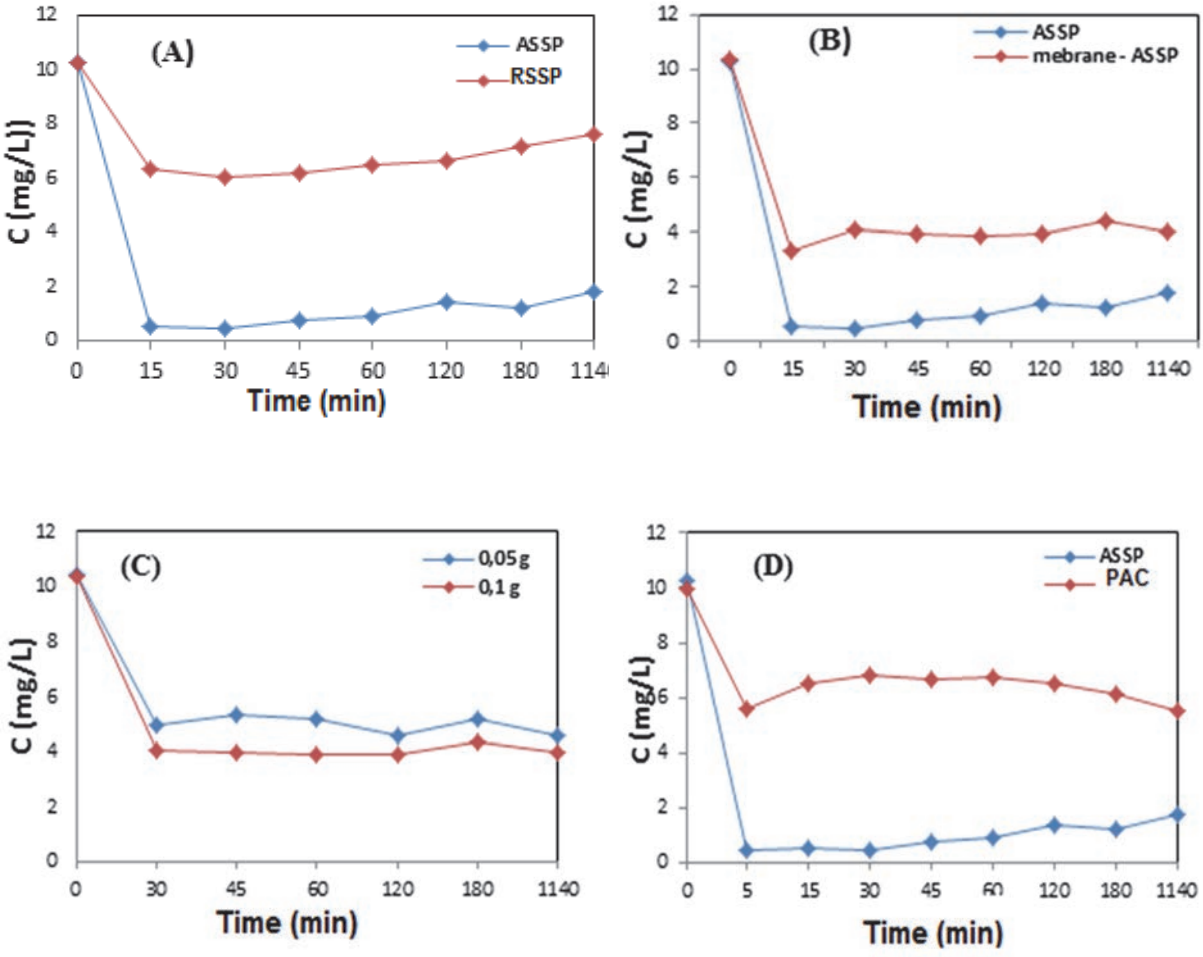

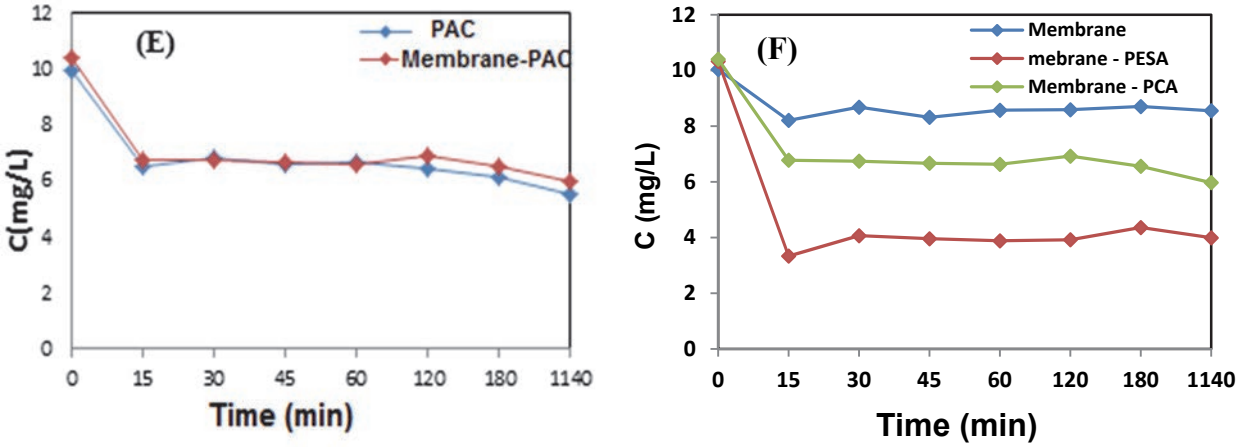

Fig. 9. Adsorption kinetics of humic substance by (A) RSSP and ASSP, (B) ASSP and ASSP/CA/PVP composite membrane, (C) different amounts of ASSP/CA/PVP, (D) ASSP and PAC , (E) PAC and PAC/CA/PVP and (F) pure CA membrane and both membranes composites

The Temkin isotherm, assumes that the heat of sorption would decrease linearly with the increase of coverage of sorbent (Temkin et al., 1940; El Haouti et al., 2019). Several authors (El Haouti et al., 2019; Doulia et al., 2009; Hank et al., 2014) propose to use this model in liquid phase. The non-linearized forms of the three isotherms are presented in Table 3 (Eqs. 3-5).

Table 3. Three Isotherm models and their non-linear forms (Thakur and Kandasubramanian, 2019)

Isotherm	*Non-linear form*	
Langmuir	$q_e = (q_m * k_L * C_e)/(1 + k_L * C_e)$	(Eq. 3)
Freundlich	$q_e = k_f * C_e^{1/n}$	(Eq. 4)
Temkin	$q_e = B_t * \ln(kt * C_e),\ B_t = R*T/\Delta G^O$	(Eq. 5)

where: q_e (mg/g), is the adsorption capacity at equilibrium, C_e (mg/L) is the sorbate equilibrium concentration, K_L (L/mg) is the Langmuir constant related to the energy of adsorption (El Haouti et al., 2018; Hank et al., 2014), and q_{max} (mg/g) the maximum adsorption capacity.

The dimensionless separation factor (R_L) is the essential characteristics of Langmuir isotherm which is expressed as equation (Eq. 6) (El Haouti et al., 2019):

$$R_L = 1/(1 + K_L * C_0) \quad (6)$$

where: C_0 is the initial concentration of sorbet in solution (mg/L). The value of R_L defines the adsorption nature as following (Table 4) (El Haouti et al., 2019):

Table 4. The value of R_L defines the adsorption nature

$R_L > 1$	Unfavorable
$R_L = 1$	Linear
$0 < R_L < 1$	Favorable
$R_L = 0$	Irreversible

K_F is the Freundlich constant (mg/g).(L/mg)$^{1/n}$, while n is an empirical constant related to the magnitude of the adsorption driving force. B_t is the Temkin constant related to heat of adsorption (kJ/mol). K_t is the equilibrium binding constant (L/mol) corresponding to the maximum binding energy (El Haouti et al., 2019). R the universal gas constant (8.314 J/mol K), T is the absolute temperature (K).

All the adsorption isotherm parameters of the non-linear models tested (Table 5) were determined by minimizing the error function and using the solver add-in with Microsoft's spreadsheet, Microsoft Excel (Boudrahem et al., 2017). The error function of Chi-square, which is one of the statistical metric widely used to assess the goodness of fit between the observed experimental data with those of corresponding values predicted by model (theoretical) (Karri et al., 2017). Therefore, this Chi-square supplied a good measurement scale to weigh the goodness of fit and identify the best fit isotherm for the adsorption system. This is expressed as equation (Eq. 7):

$$\chi^2 = \sum_{i=0}^{n} (q_{e,\exp} - \overline{q}_{e,model})_i^2 / q_{e,\exp} \quad (7)$$

where $q_{e,exp}$ and $q_{e,model}$ experimental equilibrium data (mg/g) and theoretically evaluated equilibrium (mg/g) values from the model, respectively.

The fitted isotherms parameter values for non-linear method are listed in Table 5, and the model curves are plotted in Fig. 10. The equilibrium experimental data for the adsorption of the (HS) onto the ASSP/CA/PVP and PAC/CA/PVP composites membranes and the predicted values of the different models shown indicate that the shape of the isotherms is L-type according to the classification of Gilles et al (Gilles et al. 1960). Suggestion that the two adsorbents have a high affinity and there is no competition from the molecules adsorbed for adsorption sites. As seen from Table 5, the results obtained show that the correction coefficients are very good in all cases ($R^2 >$ 0.95).

However, error analysis method suggests that the Freundlich isotherm provides a well fit to the isotherm data for the adsorption of the two adsorbents. The magnitude of the exponent n gives an indication of the favourability of adsorption. It is generally stated that values in the range of (2-10) are good, (1-2) moderately difficult, and less than 1, poor adsorption characteristics (El Haouti et al., 2019). The studied materials are good adsorbents for humic substance (n > 2). Further, the higher value of K_F was 20.22 for the ASSP/CA/PVP. The maximum adsorption capacity, q_m found for ASSP/CA/PVP and PAC/CA/PVP composites membranes were 31.00 mg/g and 23.32 mg/g, respectively. The results suggest that the humic substance is favourably adsorbed by ASSP/CA/PVP composite membrane. The value of R_L was in the range of 0.102-0.054 and 0.075-0.039 for ASSP/CA/PVP and PAC/CA/PVP composites membranes, respectively indicating a favourable ($0 < R_L < 1$) HS adsorption on the both adsorbents.

Moreover, the Temkin isotherm was studied to explore the Gibbs free energy change as: $B = RT/\Delta G°$ the value of $\Delta G°$ was 0.47 kJ/mol and 0.94 kJ/ mol for ASSP/CA/PVP and PAC/CA/PVP composites membranes, respectively. ($\Delta G° < 10$ kJ/mol) indicates a physical adsorption process (Hank et al., 2014). By way of comparison, Table 6 indicates the adsorption of humic substance on various composites adsorbents from the literature.

Table 5. Isotherm parameters obtained by using non-linear method

Models	***Constants***	***Membrane-PESA***	***Membrane-PAC***
Langmuir	q_m (mg/g)	31.00	23.32
	K_L (L/mg)	1.76	2.46
	R_L	0.102-0.054	0.075-0.039
	R^2	0.997	0.995
	χ^2	0.084	0.039
Freundlich	K_f (mg/g). $(L/mg)^{1/n}$	20.22	17.53
	1/n	0.220	0.13
	n	4.56	7.58
	R_2	0.999	0.099
	χ^2	0.026	0.008
Temkin	K_t (L/mol)	46.86	709.51
	B	5.23	2.65
	$\Delta G°$ (kJ/mol)	0.47	0.94
	R^2	0.998	0.999
	χ^2	0.035	0.011

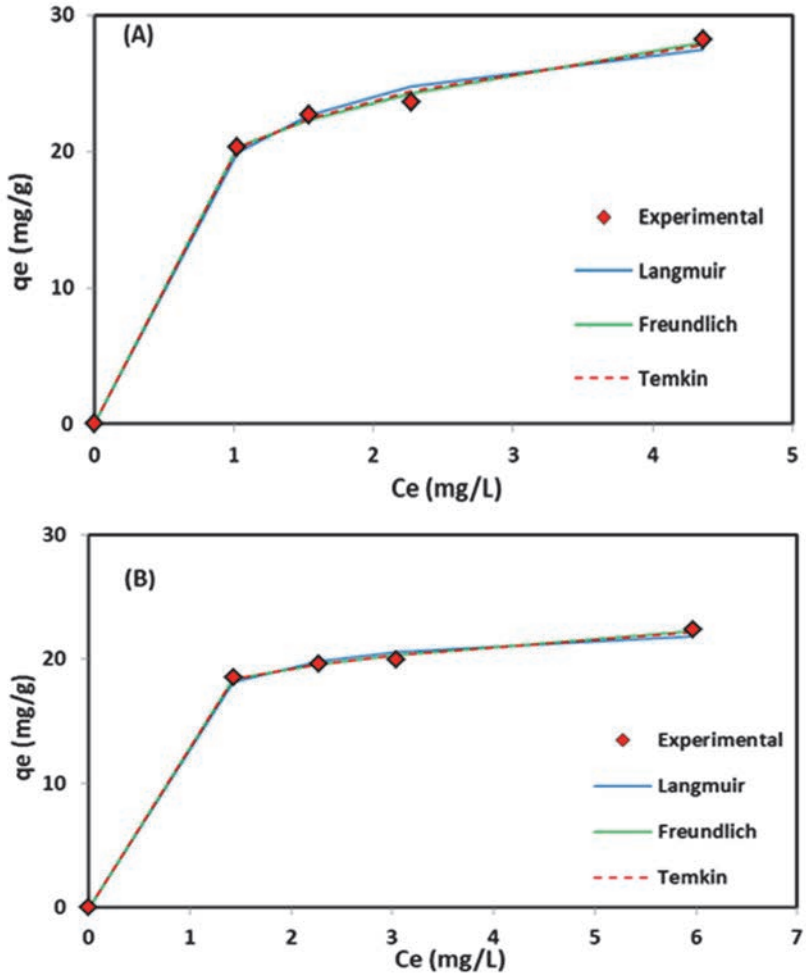

Fig. 10. Isotherms obtained using the non -linear method for the composite's membranes: (A) ASSP /CA/ PVP, (B) PAC /CA/ PVP

Table 6. Comparison of maximum humic substance adsorption capacity obtained in this study with previous data

Adsorbents	***Maximum adsorption capacities (mg/g)***	***References***
ASSP/CA/PVP composites membranes	30.00	This study
PAC/CA/PVP composites membranes	23.32	This study
Zirconia embedded in polyethersulfone membrane	50.5	Thuyavan et al. (2014)
Carbon nanotubes/polyacrylamide composites	12.52	Yang et al. (2011)
Zeolite/TiO_2	5.94	Liu et al. (2014)
Chitosan coated iron-oxide-polyacrylonitrile mixed matrix membrane	70	Panda et al. (2014)
Aminated polyacrylonitrile fibers (APANFs)	16.22	Deng and Bai (2004)

4. Conclusions

This study has shown the performance of ASSP /CA/ PVP and PAC /CA/ PVP composites membranes prepared by phase inversion in removal efficiency of HS. The membranes morphologies using SEM shows that the pores development amplified with the integration of both materials ASSP and PAC to the pure polymer (CA/PVP). ASSP /CA/ PVP composite membranes are more porous compared with PAC/CA/PVP composite; this higher porosity leads to more efficiency in elimination of humic substance.

The adsorption isotherm non-linear data fit to Freundlich model. The value of $\Delta G°<10$ kJ/mol indicates a physical adsorption process.

The maximum monolayer adsorption capacity (q_{max}) for the prepared ASSP/CA/PVP was found to be higher (31.00 mg/g) than the PAC/CA/PVP (23.32 mg/g). The results showed in this work indicated that ASSP /CA/ PVP composite membrane is a promising material for humic substances removal from aqueous solutions.

References

Abd El-aziz A.M., El-Maghraby A., Taha N.A., (2017), Comparison between polyvinyl alcohol (PVA) nanofiber and polyvinyl alcohol (PVA) nanofiber/hydroxyapatite (HA) for removal of Zn2+ions from wastewater, *Arabian Journal of Chemistry*, **10**, 1052-1060.

Arthanareeswaran G., Sriyamuna Devi TK., Raajenthiren M., (2008), Effect of silica particles on cellulose acetate blend ultrafiltration membranes: Part I, *Separation and Purification Technology*, **64**, 38-47.

Basri M., Ahmad M.B., Shameli K., Khandanlou R., Kalantari K., Fard Masoumi H.R., (2014), Rapid and high capacity adsorption of heavy metals by Fe_3O_4/montmorillonite nanocomposite using response surface methodology: Preparation, characterization, optimization, equilibrium isotherms, and adsorption kinetics study, *Journal of the Taiwan Institute of Chemical Engineers*, **49**, 192-198.

Beddow H., Black S., Read D., (2006), Naturally occurring radioactive material (NORM) from a former phosphoric acid processing plant, *Journal of Environmental Radioactivity*, **86**, 289-312.

Boudrahem N., Delpeux-Ouldriane S., Khenniche L., Boudrahem F., Aissani-Benissad F., Gineys M., (2017), Single and mixture adsorption of clofibric acid, tetracycline and paracetamol onto activated carbondeveloped from cotton cloth residue, *Process Safety and Environmental Protection*, **111**, 544-559.

Celik E., Park H., Choi H., Choi H., (2011), Carbon nanotube blended polyethersulfone membranes for fouling control in water treatment, *Water Research*, **45**, 274-282.

Corami A., Mignardi S., Ferrini V., (2007), Copper and zinc decontamination from single-and binary-metal solutions using hydroxyapatite, *Journal of Hazardous Materials*, **146**, 164-170.

Doulia D., Leodopoulos C., Gimouhopoulos K., Rigas F., (2009), Adsorption of humic acid on acid-activated Greek bentonite, *Journal of Colloid and Interface Science*, **340**, 131-141.

El Haouti R., Anfar Z., Chennah A., Amaterz E., Zbair M., El Alem N., Benlhachemi A., Ezahri M., (2019), Synthesis of sustainable mesoporous treated fish waste as adsorbent for copper removal, *Groundwater for Sustainable Development*, **8**, 1–9.

Fernando M.S., De Silva R.M., De Silva K.M.N., (2015), Synthesis, characterization and application of nano hydroxyapatite and nanocomposite of hydroxyapatite with granular activated carbon for the removal of $Pb2^+$ from aqueous solutions, *Applied Surface Science*, **351**, 95-103.

Freundlich H.M.F., (1906), Over the adsorption in solution, *The Journal of Physical Chemistry*, **57**, 385-471.

Ghaedi M., Khafri H.Z., Asfaram A., Goudarzi A., (2016), Response surface methodology approach for optimization of adsorption of Janus Green B from aqueous solution onto ZnO/Zn(OH)<inf>2</inf>-NP-AC: Kinetic and isotherm study, *Spectrochimica Acta-Part A: Molecular and Biomolecular Spectroscopy*, **152**, 233-240.

Gilles C.H., McEwan J.H., Nakwa S.N., Smith D., (1960), Studies in adsorption. Part XI. A system of classification of solution adsorption isotherms, and its use in diagnosis of adsorption mechanisms and in measurement of specific surface areas of solids, *Journal of the Chemical Society (London)*, **3**, 3973-3993.

Hamdaoui O., Naffrechoux E., (2007), Modeling of adsorption isotherms of phenol and chlorophenols onto granular activated carbon. Part I. Two-parameter models and equations allowing determination of thermodynamic parameters, *Journal of Hazardous Materials*, **147**, 381-394.

Hank D., Azi Z., Ait Hocine S., Chaalal O., Hellal A., (2014), Optimization of phenol adsorption onto bentonite by factorial design methodology, *Journal of Industrial and Engineering Chemistry*, **20**, 2256-2263.

Harfouchi H., Hank D., Hellal A., (2016), Response surface methodology for the elimination of humic substances from water by coagulation using powdered Saddled sea bream scale as coagulant-aid, *Process Safety and Environmental Protection*, **99**, 216-226.

He F., Ren Z., Sun X., Wang Y., Yan Y., Li Q., Wang L., (2015), Recycling flue gas desulphurization (FGD) gypsum for removal of Pb(II) and Cd(II) from wastewater, *Journal of Colloid and Interface Science*, **457**, 86-95.

Huang Y.C., Hsiao P.C., Chai H.J., (2011), Hydroxyapatite extracted from fish scale: Effects on MG63 osteoblast-like cells, *Ceramics International*, **37**, 1825-1831.

Hwang L.L., Chen J.C., Wey M.Y., (2013), The properties and filtration efficiency of activated carbon polymer composite membranes for the removal of humic acid, *Desalination*, **313**, 166-175.

Hwang L.L., Wey M.Y., Chen J.C., (2014), Effects of membrane compositions and operating conditions on the filtration and backwashing performance of the activated carbon polymer composite membranes, *Desalination*, **352**, 181-189.

Karri R.R., Sahu J.N., Jayakumar N.S., (2017), Optimal isotherm parameters for phenol adsorption from aqueous solutions onto coconut shell based activated carbon: Error analysis of linear and non-linear methods, *Journal of the Taiwan Institute of Chemical Engineers*, **80**, 472-487.

Kontrec J., Kralj D., Brečević L., (2003), Cadmium removal from calcium sulphate suspension by liquid membrane extraction during recrystallization of calcium sulphate anhydrite, *Colloids and Surfaces A: Physicochemical and Engineering Aspects*, **223**, 239-249.

Koopman C., Witkamp G.J., (2000), Extraction of lanthanides from the phosphoric acid production process to gain a purified gypsum and a valuable lanthanide by-product, *Hydrometallurgy*, **58**, 51-60.

Langmuir I., (1918), The adsorption of gases on plane surfaces of glass, mica and platinum, *Journal of the American Chemical Society*, **40**, 1361-1403.

Liu S., Lim M., Amal R., (2014), TiO2-coated natural zeolite: rapid humic acid adsorption and effective photocatalytic regeneration, *Chemical Engineering Science*, **105**, 46-52.

Maldhure A.V., Ekhe J.D., (2011), Preparation and characterizations of microwave assisted activated carbons from industrial waste lignin for Cu(II) sorption, *Chemical Engineering Journal*, **168**, 1103-1111.

Mohamad Said K.A., George G.G., Mohamed Alipah N. A., Ismail N.Z., Jama'in R.L., Mili N., Salleh S.F., Mohamed Amin M.A., Muslimen R., Yakub I., Mohamed Sutan N., (2017), Effect of activated carbon in polysufone-polyethyleneimine-silver composite membrane towards adsorption of chromium (Cr), lead (Pb), silver (Ag) and cadmium (Cd) in synthetic wastewater, *Journal of Materials and Environmental Science*, **8**, 3740-3746.

Mohammadi T., Saljoughi E., (2009), Effect of production conditions on morphology and permeability of asymmetric cellulose acetate membranes, *Desalination*, **243**, 1-7.

Mota J.A., Chagas R.A., Vieira E.F.S., Cestari A.R., (2012), Synthesis and characterization of a novel fish scale-immobilized chitosan adsorbent-Preliminary features of dichlorophenol sorption by solution calorimetry, *Journal of Hazardous Materials*, **229-230**, 346-353.

Önal M., Sarikaya Y., (2007), Preparation and characterization of acid-activated bentonite powders, *Powder Technology*, **172**, 14-18.

Pantos M., Nicholson J., Almond M.J., Matthews W., Shillito L.M., (2009), Rapid characterisation of archaeological midden components using FT-IR spectroscopy, SEM–EDX and micro-XRD, *Spectrochimica Acta Part A: Molecular and Biomolecular Spectroscopy*, **73**, 133-139.

Rahimpour A., Madaeni S.S., (2007), Polyethersulfone (PES)/cellulose acetate phthalate (CAP) blend ultrafiltration membranes: Preparation, morphology, performance and antifouling properties, *Journal of Membrane Science*, **305**, 299-312.

Rajeswari A., Amalraj A., Pius A., (2015), Removal of phosphate using chitosan-polymer composites, *Journal of Environmental Chemical Engineering*, **3**, 2331-2341.

Ramakrishnan P., Nagarajan S., Thiruvenkatam V., Palanisami T., Naidu R., Mallavarapu M. ,Rajendran S., (2016), Cation doped hydroxyapatite nanoparticles enhance strontium adsorption from aqueous system: A comparative study with and without calcination, *Applied Clay Science*, **134**, 136-144.

Saljoughi E., Mohammadi T., (2009), Cellulose acetate (CA)/polyvinylpyrrolidone (PVP) blend asymmetric membranes: Preparation, morphology and performance, *Desalination*, **249**, 850-854.

Saljoughi E., Sadrzadeh M., Mohammadi T., (2009), Effect of preparation variables on morphology and pure water permeation flux through asymmetric cellulose acetate membranes, *Journal of Membrane Science*, **326**, 627-634.

Techawongstien S., Buapa K., Janpradit K., Kongsri S., Chanthai S., (2012), Nanocrystalline hydroxyapatite from fish scale waste: Preparation, characterization and application for selenium adsorption in aqueous solution, *Chemical Engineering Journal*, **215-216**, 522-532.

Temkin M.I., Pyzhev V., (1940), Kinetic of ammonia synthesis on promoted iron catalyst, *Acta Physicochimica U.R.S.S*, **12**, 327-356.

Thakur K., Kandasubramanian B., (2019), Graphene and graphene oxide-based composites for removal of organic pollutants: A review, *Journal of Chemical and Engineering Data*, **64**, 833-867.

Thuyavan Y.L., Anantharaman N., Arthanareeswaran G., Ismail A.F., (2014), Adsorptive removal of humic acid by Zirconia embedded in polyethersulfone membrane, *Industrial and Engineering Chemistry Research*, **53**, 11355-11364.

Ulu F., Barişçi S., Kobya M., Särkkä H., Sillanpää M., (2014), Removal of humic substances by electrocoagulation (EC) process and characterization of floc size growth mechanism under optimum conditions, *Separation and Purification Technology*, **133**, 246-253.

Wei W., Yang L., Zhong W., Cui J., Wei Z., (2015), Poorly crystalline hydroxyapatite: A novel adsorbent for enhanced fulvic acid removal from aqueous solution, *Applied Surface Science*, **332**, 328-339.

Williams M.D., Ravindran V., Pirbazari M., (2012), Modeling and process evaluation of membrane bioreactor for removing biodegradable organic matter from water, *Chemical Engineering Science*, **84**, 494-511.

Wu G., Gan S., Cui L., Xu Y., (2008), Preparation and characterization of PES/TiO_2 composite membranes, *Applied Surface Science*, **254**, 7080-7086.

Yang S., Hu J., Chen C., Shao D., Wang X., (2011), Mutual effects of Pb (II) and humic acid adsorption on multiwalled carbon nanotubes/polyacrylamide composites from aqueous solutions, *Environmental Science and Technology*, **45**, 3621-3627.

Zhao S., Gao B., Yue Q., Song W., Jia R., Liu P., (2015), Evaluation of floc properties and membrane fouling in coagulation-ultrafiltration system: The role of *Enteromorpha polysaccharides*, *Desalination*, **367**, 126-133.